Mechanical Properties on Electron Beam Welds of Constructional High Tension Steels (Report I)†

Yoshiaki ARATA*, Fukuhisa MATSUDA, Yutaka SHIBATA***, Shigeomi HOZUMI***, Yoshihisa ONO*** and Shouichiro FUJIHIRA******

Abstract

Square-butt welding was performed on 25 mm thick plates of commercial high tension steels (HT-50, 60 and 80) with electron-beam welding. Two electron-beam welders (conventional high voltage and low voltage types) were used on this investigation and weld heat input was respectively varied with and without preheating.

Some results of the mechanical properties of the welds of HT—50, 60 and 80 steels such as hardness distribution, tensile and impact properties were investigated in this paper.

Most of welds have had no defects that were detectable by dye penetrant and X-ray inspections. It seemed that only Mn in welds was a little vaporized during electron-beam welding. The maximum hardness of welds was decreased with the adoption of preheating but even in the welds without preheating it was not so high to originate the cold cracks.

Most of tensile-tested specimens for the welded joint fractured in the base metal, and all of face and root bended showed the complete bend angle of 180 degrees without any defects.

Impact strength of welded joints showed adequate value in HT—60 and 80 steels, but inadequate value in some of weld metals of HT—50 in comparison with the criteria of JIS (Japanese Industrial Standard) and WES (Welding Engineering Standard) Specifications. However the results of these mechanical tests indicate that the electron-beam welds in these high tension steels will be anticipated in practical use for many fields of application,

1. Introduction

By use of electron-beam with high power density, the electron beam welding is performed for thicker plates with high speed. As the power density of electron-beam is higher than that of conventional arc heat source, extremely a narrow and deep penetrated bead and small quantity of distortion in welded joint is obtained. Furthermore, the additional benefit of electron-beam welding is that the molten weld metal is free from atmospheric gases of oxygen, nitrogen and moisture owing to vacuum. On the other hand, as compared with the conventional arc welding methods, the cooling rate of molten metal for electron-beam welding is much higher. Namely, time of chemical reaction in fusion zone during welding is extremely short because of a small weld heat input in electron-beam welding.

Then, the release of gases and impurities from the molten metal before solidification is not sufficiently accomplished, and therefore the weld defects occur often. Therefore, electron beam welding must be carefully conducted because the weldability of electron-beam welds is still unknown.

There are few data[1),2)], so far, concerning the mechanical characteristics of the high tension steels which are used in constructions as bridge, building, tower and so on. Then, in this investigation, the authors aimed to make clear the mechanical properties on the electron-beam welds for commercial constructional high tension steels as HT—50, HT—60 and HT—80. The authors treated here about tensile, bending and impact properties of these welds as the first stage.

2. Experimental Procedure

2.1 Materials used

The materials used in this investigation are HT—50, HT—60 and HT—80 steels which are widely used in the constructional bridges and buildings. The chemical compositions of these three types of high tension steel are listed in **Table 1.** 25 mm thick plates of these steels were square butt-welded with electron-beam welding processes.

2.2 Welding condition

(1) Electron-beam welders

† Received on July 22, 1974

* Professor
** Associate Professor
*** Katayama Iron Works, Ltd.
**** Co-operative researcher (1974), Katayama Iron Works, Ltd.

Table 1. Chemical composition of HT—50, 60 and 80 steels.

(wt%)

Composition / Steel	C	Si	Mn	P	S	Ni	Cr	Mo	V	Ceq*
HT—50	0.18	0.43	1.54	0.027	0.021	0.028	0.019	0.002	0.004	0.46
HT—60	0.13	0.32	1.32	0.015	0.013	0.025	0.012	tr	0.030	0.37
HT—80	0.13	0.29	0.85	0.016	0.008	0.98	0.48	0.39	0.023	0.50

*: $Ceq=C+\frac{1}{6}Mn+\frac{1}{24}Si+\frac{1}{40}Ni+\frac{1}{5}Cr+\frac{1}{4}Mo+\frac{1}{14}V$ (JISZ 3106)

Table 2. Capacities of high and low voltage type electron-beam welders.

	High voltage type electron-beam welder	Low voltage type electron-beam welder
Maximum beam power	150—40 (KV-mA) =6 (KW)	30—500 (KV-mA) =15 (KW)
Chamber size	1.0 m (Width) ×1.0 m (Height) ×1.3 m (Length)	1.0 m (Width) ×1.0 m (Height) ×2.0 m (Length)
Vacuum of chamber during welding	10^{-4} (mm Hg)	10^{-4} (mm Hg)
Filament	Hair pin-type (Tungsten used)	plate-type (Tantalum used)

All of welding in this investigation were done by using two types of conventional high and low voltage electron-beam welders. **Table 2** shows the capacities of two types of electron-beam welder used in this investigation.

(2) Welding procedure

Welding for all materials to be treated was performed for one pass or two passes without and with preheating of 100°C under the joint profile of butt type as shown in **Fig. 1.** The size of the specimens is 200 mm in width, 500 mm in length and 25 mm in thickness, and each two specimens is welded in longitudinal seam. The welding conditions used on various materials are given in **Table 3.** The beam active parameters[3] a_b, was respectively selected for 0.97 and 0.93 in high and low voltage electron-beam welders. Every square butt joint had a good fitup and did not have any excessive gap and misalignment by use of restraint jig and tack welding. Root faces of joint for the electron-beam welding were completely machined to have no seam gap, and the scale on both plate surfaces was also eliminated along the welding direction with the width of 10 mm from the seam. All of the specimens used in this investigation were completely de-magnetized, and the root faces of joint were made clean by acetone in advance of electron-beam welding.

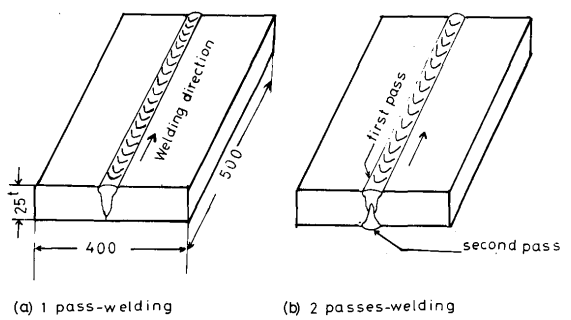

Fig. 1. Dimension of specimen.

The following shows the additional notes in welding performance.

a) Welding conditions, A and C for the one pass-welding were selected from the result of preliminary test, the weld heat input of which was burnt through 20 mm thick steel plate, and welding conditions, B and D for the two passes-welding were also selected as the weld heal input to burn through 15 mm thick steel plate.

b) 100°C preheating was performed by driving the defocused electron-beam along the welding line by three times, the electron beam of which was about 20 mm in diam. Preheating temperature, 100°C was recognized by use of a chromel-alumel thermocouples.

c) In case of two passes-welding, the raised temperature in welded joint due to the first pass-welding with or without preheating was fully cooled to R·T

Table 3. Welding condition.

Condition / Series	Beam power (KV-mA)	Welding speed (cm/min)	Preheat temp. (°C)	Welding procedure
D5A, D6A, D8A	150—33 ≒(5 KW)	15	R·T	one pass-welding as Fig. 1 (a)
D5B, D6B, D8B	150—33 ≒(5KW)	24	R·T	two passes-welding as Fig. 1 (b)
D5C, D6C, D8C	150—33 ≒(5 kW)	15	100	one pass-welding as Fig. 1 (a)
D5D, D6D, D8D	150—33 ≒(5 KW)	24	100	two passes-welding as Fig. 1 (b)
N5A, N6A, N8A	30—250≒(7.5 KW)	30	R·T	one pass-welding as Fig. 1 (a)
N5B, N6B, N8B	30—250≒(7.5 KW)	60	R·T	two passes-welding as Fig. 1 (b)
N5C, N6C, N8C	30—250≒(7.5 KW)	30	100	one pass-welding as Fig. 1 (a)
N5D, N6D, N8D	30—250≒(7.5 KW)	60	100	two passes-welding as Fig. 1 (b)

Note; D; High voltage type E·B-welder
N; Low voltage type E·B-welder
5 ; HT50 6; HT60 8; HT80
A, B, C, D; Welding condition

before the second pass-welding. Then the second pass was performed without and with 100°C preheating. Both the first and the second passes were welded in the same direction.

3. Experimental Results

3.1 Non-destructive inspection

1) X-ray inspection

All of the electron-beam welds of high tension steels were X-ray inspected. Any defect such as porosity and crack could not be detected in the electron-beam welds of HT—50, 60 and 80 steels. Referring to JIS Specification (JIS Z 3104—1968), most of electron-beam welds were allowable in the first class for general grade.

2) Dye penetrant inspection

All of the weld surfaces of high tension steels were also checked by dye penetrant test. No surface defects were observed at all in all electron-beam welds.

3.2 Chemical analysis of weld metal

Table 4 shows the results of the quantitative

Table 4. Chemical analysis of weld metal.

(wt.%)

Steel		C	Si	Mn	P	S
HT—50	Base metal	0.18	0.43	1.54	0.027	0.021
	D5A— weld metal	0.19	0.42	1.23	0.028	0.021
	N5A— weld metal	0.18	0.45	1.29	0.026	0.021
HT—60	Base metal	0.13	0.32	1.32	0.015	0.013
	D6A— weld metal	0.14	0.36	1.06	0.016	0.014
	N6A— weld metal	0.15	0.36	1.14	0.016	0.015
HT—80	Base metal	0.13	0.29	0.85	0.016	0.008
	D8A— weld metal	0.14	0.32	0.69	0.015	0.008
	N8A— weld metal	0.13	0.28	0.70	0.014	0.005

analysis of C, Si, Mn, P and S for the one pass-welds of HT—50, 60 and 80 steels after welding. Regardless of the difference of the electron beam welder, only Mn in the welds is clearly decreased to that in the base metal. It seems that Mn in the welds vaporizes during electron-beam welding, as the partial pressure of Mn is high enough in calculation in molten metal during welding[4].

3.3 Metallographic and hardness examinations

1) Metallographic examinations

Macrophotographs and microphotographs of the entire welds for HT—60 steels are shown in **Photo. 1,** which were welded with one pass and two passes by high voltage type electron-beam welder. The welds have a typical cast structure with rapid solidification, and the cellular dendrites are extremely small. As welding speed decreases to 15 cm/min, the cellular structure parallel to the welding direction is observed in the center of weld bead as shown in upper Photo. 1. Preheating did not show any obvious effect upon variation of the microstructures.

2) Hardness examinations

Harkness distribution was measured in each cross-section of the welds using Vickers hardness tester with 1 kg load. Vickers hardness distributions of welds for HT—50, 60 and 80 steels using low voltage-type welder are respectively shown in **Figs. 2, 3** and **4.** It is anticipated in general that the hardness must be maximum at the weld metal because the cooling rate is theoretically the highest in the temperature range to be quenched. However the weld metal was usually softer

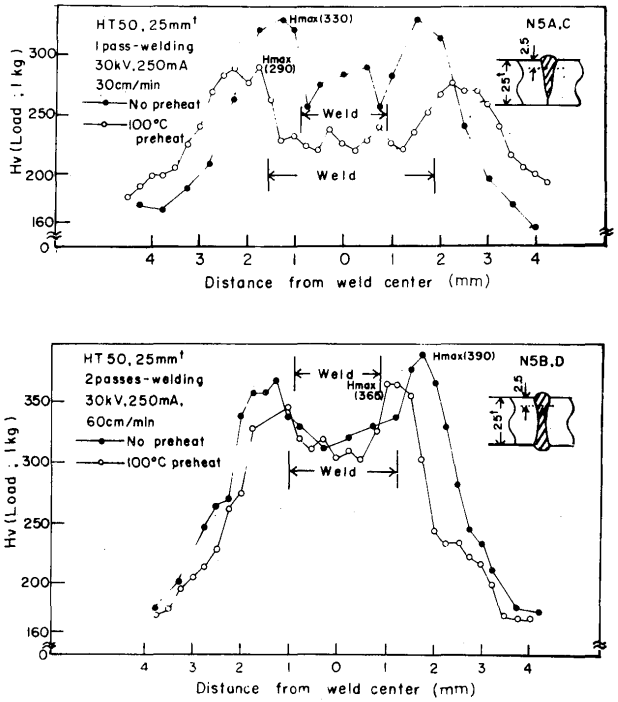

Fig. 2. Vickers hardness distribution of welds for HT—50 steel using low voltage type E·B welder.

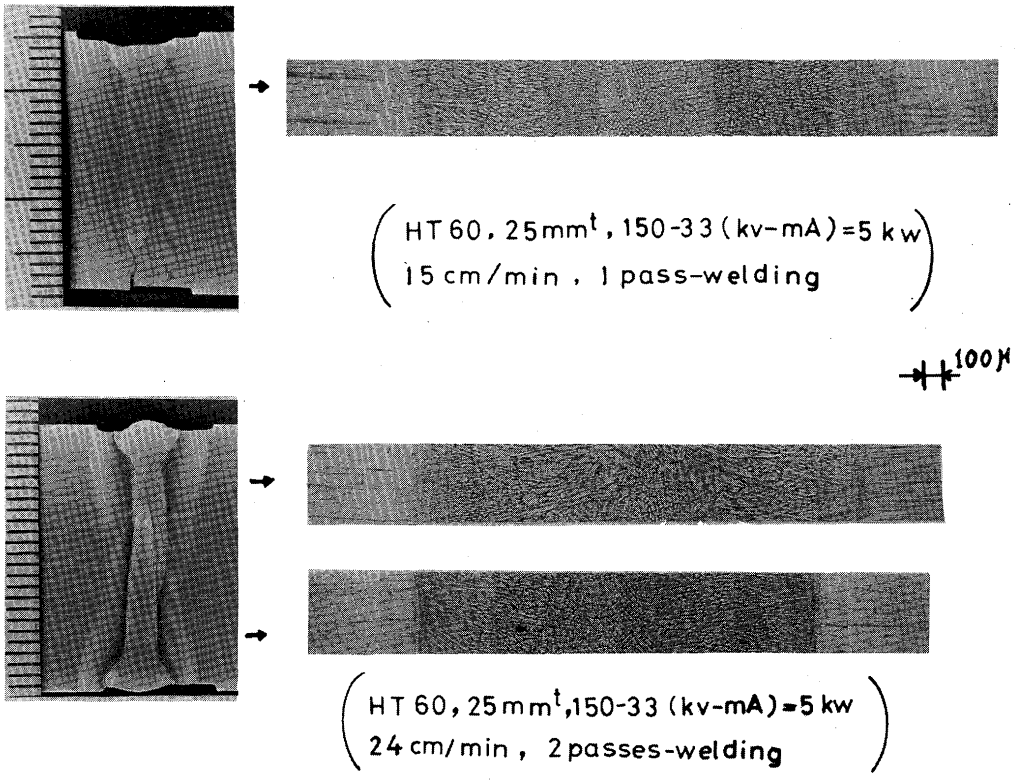

Photo. 1. Macro and microphotographs of welds without preheating for HT—60 steel by use of high voltage type E·B welder.

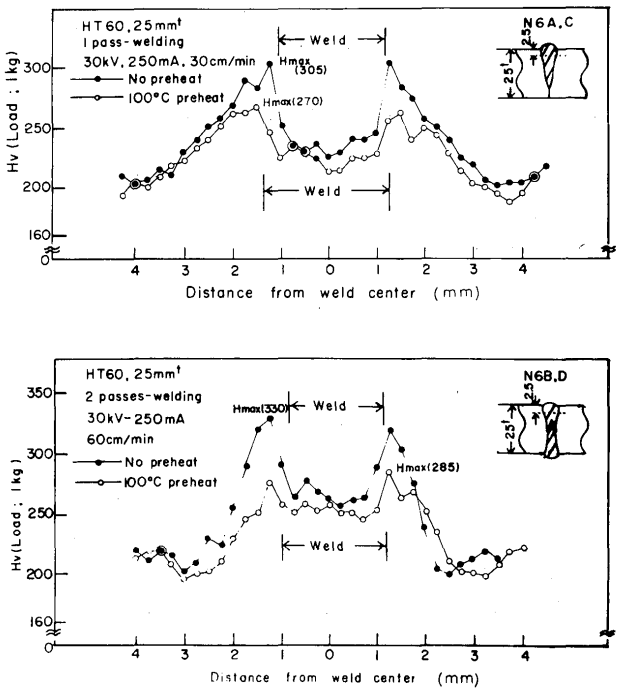

Fig. 3. Vickers hardness distribution of welds for HT—60 steel using low voltage type E·B welder.

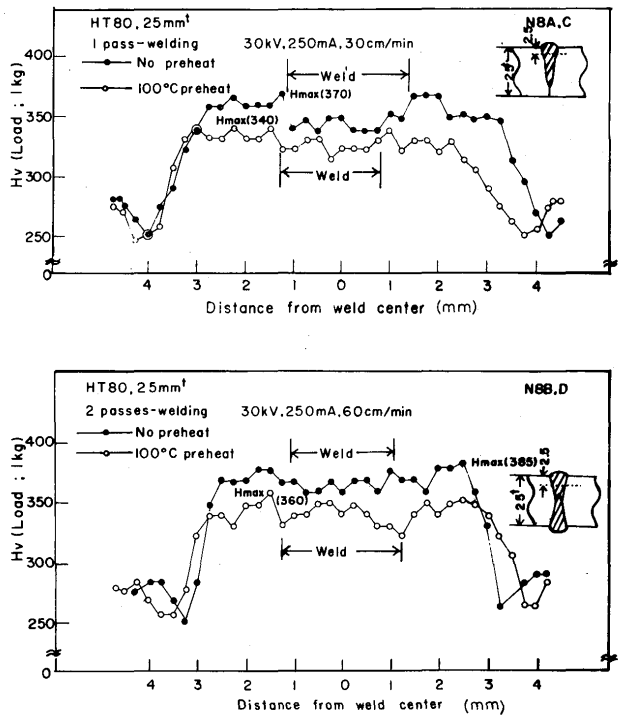

Fig. 4. Vickers hardness distribution of welds for HT—80 steel using low voltage type E·B welder.

than the HAZ near fusion boundary as shown in Figs. 2, 3 and 4. The authors think that it is due to the vaporization of Mn element which is analysed in Table 4. Furthermore, the hardnesses of welds with 100°C preheating usually showed lower value than that of the welds without preheating for both one pass and two passes-welding.

Figs. 5, 6 and **7** respectively show the relations between the weld heat input and hardness of welds for HT—50, 60 and 80 steels. Hw is the average hardness of weld metal and Hmax is the maximum hardness of welds which usually occurs in the HAZ. It is found that the hardness of welds decreases with an increase of weld heat input. This tendency shows irrespective of the difference of electron-beam welder.

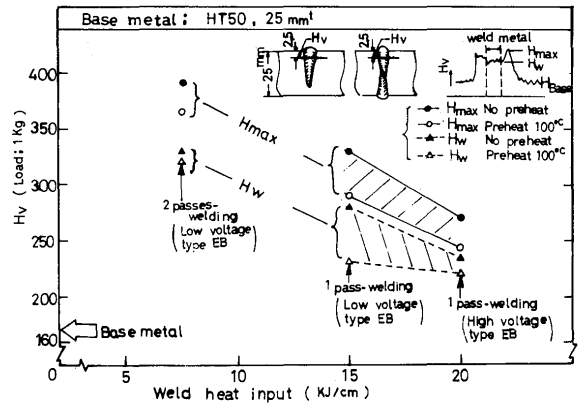

Fig. 5. Relation between weld heat input and hardness of welds for HT—50 steel.

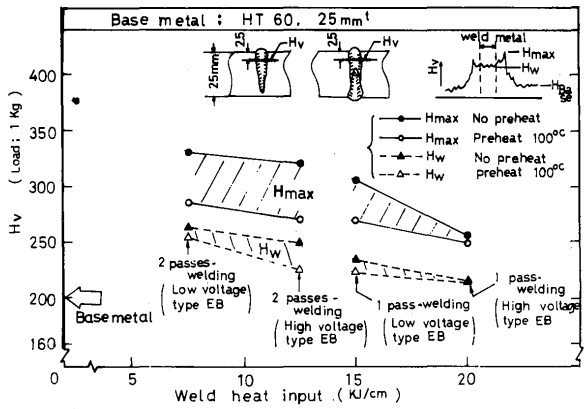

Fig. 6. Relation between weld heat input and hardness of welds for HT—60 steel.

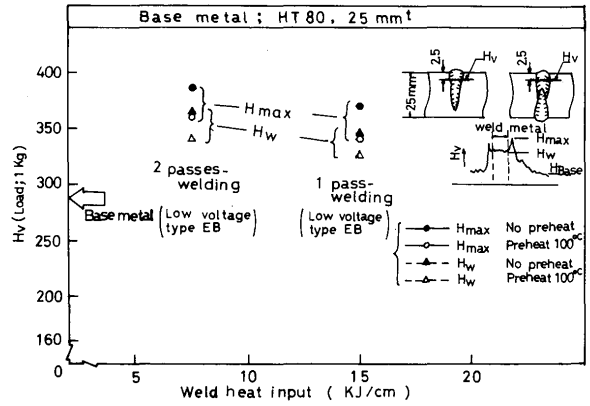

Fig. 7. Relation between weld heat input and hardness of welds for HT—80 steel.

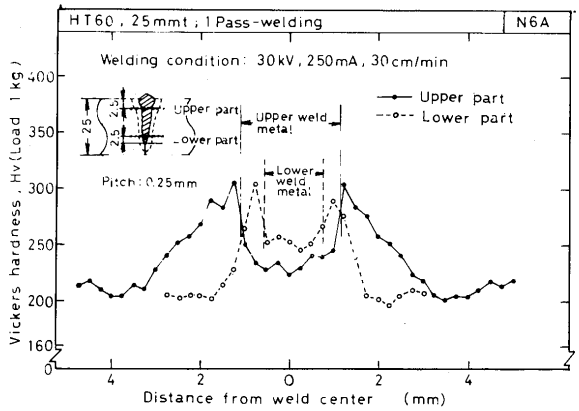

Fig. 8. Difference of Vickers hardness distribution between upper and lower part of weld metal for one pass-welding.

Namely it results that the hardness of welds is directly related to the cooling rate. Furthermore, as shown in **Fig. 8,** the hardnesses in the lower part of weld metal for one pass-welding usually show higher value than those of the upper part, which is due to the difference of cooling rate.

3.4 Tensile test results

Two types of uniaxial tensile test specimen were made from the welded high tension steels of HT—50, 60 and 80, the lengths of the parallel part of which were 220 mm and 12 mm, respectively as shown in **Fig. 9** (a) and (b). Two specimens were examined for each welding condition in the respective tensile test.

An example of the two types of tested specimens for HT—50 is shown in **Photo. 2.** In case of 220 mm parallel length, all of the tensile tested specimens were fractured in base metal. Meanwhile, in case of 12 mm

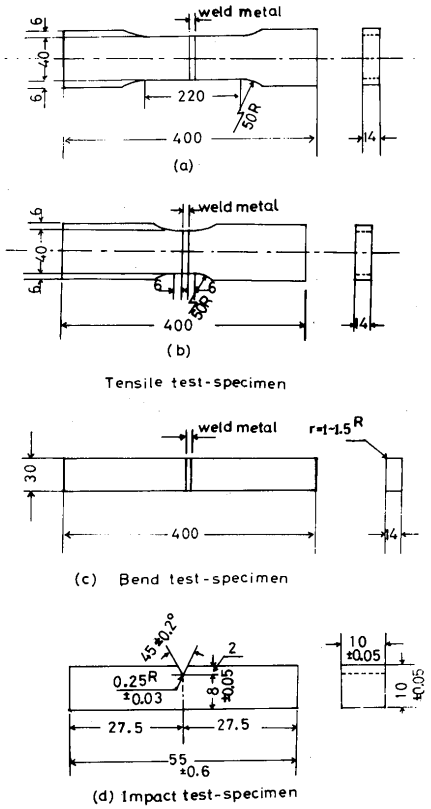

Fig. 9. Dimension of each test specimen.

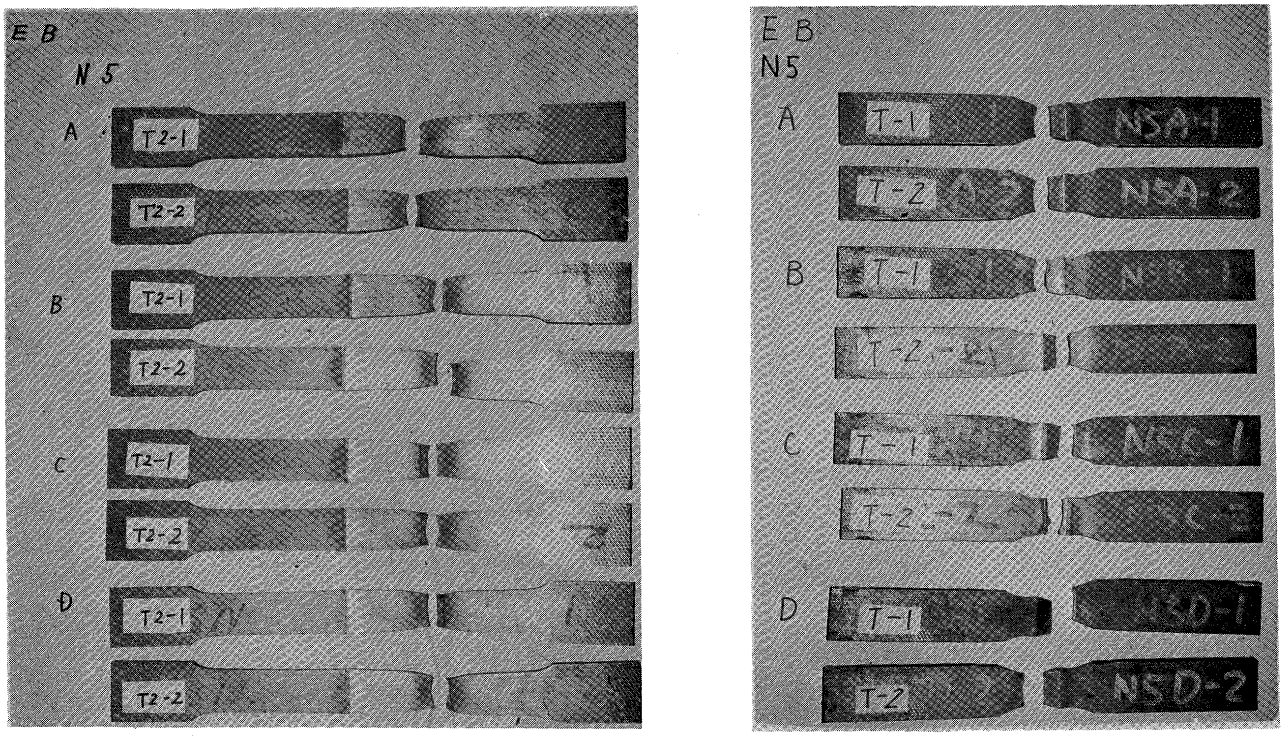

(a) (b)

Photo. 2. An example of two types of tested specimens for HT—50 steel.
(a) Length of parallel part: 220 mm (b) Length of parallel part: 12 mm

parallel length, two specimens were fractured in the welds but the tensile strengths of them were equal to those of the other specimens which were fractured in base metal. The tensile test results are tabulated in **Tables 5** and **6.** Specimen number in those tables corresponds to the welding condition in Table 3.

Table 5. Tensile test results (Length of parallel part; 220 mm).

Steel	Specimen number	Tensile Strength, σ_T (kg/mm^2)	Elongation in GL: 100 mm (%)	Fractured in
HT—50	D5A—1	56.7	20	Base metal (BM)
	A—2	56.7	24	〃
	D5B—1	56.4	—	〃
	B—2	56.9	—	〃
	D5C—1	56.7	—	〃
	C—2	56.3	—	〃
	D5D—1	57.1	—	〃
	D—2	56.7	—	〃
	N5A—1	53.9	—	BM
	A—1	54.8	—	〃
	N5B—1	55.0	—	〃
	B—2	55.5	—	〃
	N5C—1	55.1	—	〃
	C—2	54.4	—	〃
	N5D—1	54.5	—	〃
	D—2	53.4	—	〃
HT—60	D6A—1	60.3	—	BM
	A—2	58.5	—	〃
	D6B—1	57.9	—	〃
	B—2	58.0	—	〃
	D6C—1	58.7	—	〃
	C—2	58.1	—	〃
	D6D—1	57.9	23	〃
	D—2	58.3	—	〃
	N6A—1	59.8	20	BM
	A—2	59.8	—	〃
	N6B—1	59.7	—	〃
	B—2	59.9	21	〃
	N6C—1	60.0	—	〃
	C—2	60.9	—	〃
	N6D—1	59.8	20	〃
	D—2	59.0	—	〃
HT—80	D8A—1	89.5	13	BM
	A—2	89.8	—	〃
	D8B—1	86.2	12	〃
	B—2	85.7	—	〃
	D8C—1	89.2	—	〃
	C—2	88.7	12	〃
	D8D—1	88.7	—	〃
	N8A—1	86.7	13	BM
	N8B—1	86.9	12	〃
	B—2	87.3	13	〃
	N8C—1	87.3	13	〃
	C—2	86.8	—	〃
	N8D—1	86.6	—	〃
	D—2	87.2	—	〃

Table 6. Tensile test results (Length of parallel part; 12 mm).

Steel	Specimen number	Tensile strength, σ_T (kg/mm^2)	Fractured in
HT—50	D5A—1	64.4	Base metal (BM)
	A—2	65.0	〃
	D5B—1	64.4	〃
	B—2	64.6	〃
	D5C—1	65.2	〃
	C—2	64.3	〃
	D5D—1	65.2	〃
	D—2	64.1	〃
	N5A—1	62.5	BM
	A—2	63.2	〃
	N5B—1	61.8	〃
	B—2	61.0	〃
	N5C—1	62.8	〃
	C—2	62.4	Weld metal
	N5D—1	61.7	BM
	D—2	61.5	〃
HT—60	D6A—1	66.2	BM
	A—1	65.4	〃
	D6B—1	65.0	〃
	B—2	65.4	〃
	D6C—1	64.4	〃
	C—2	64.4	〃
	D6D—1	64.5	〃
	D—2	65.1	〃
	N6A—1	67.3	BM
	A—2	66.7	〃
	N6B—1	66.0	〃
	B—2	65.4	〃
	N6C—1	66.7	〃
	C—2	65.7	〃
	N6D—1	66.9	〃
	D—2	66.1	〃
HT—80	D8A—1	98.3	BM
	A—2	97.2	〃
	D8B—1	92.6	〃
	B—1	92.6	〃
	D8C—1	96.4	〃
	C—2	96.9	〃
	D8D—1	95.0	〃
	N8A—1	97.1	HAZ
	N8B—1	95.8	BM
	B—2	95.1	〃
	N8C—1	98.0	〃
	C—2	99.1	〃
	N8D—1	96.4	〃
	D—2	96.0	〃

3.5 Bend test results

Roller bend test (bend radius; 24 mm) was made for the welded joints (HT—50, 60 and 80) with the bend test specimens as shown in Fig. 9 (c). Two specimens were prepared for one welding condition, and one of them was face bend tested and the other was root bend tested. An example of bend tested-specimens is shown in **Photo. 3.** All of the face and the root bend tested specimens showed the complete bend angle of 180 degrees without any crack, but extremely small defect was observed on the surface of two root bend tested specimens.

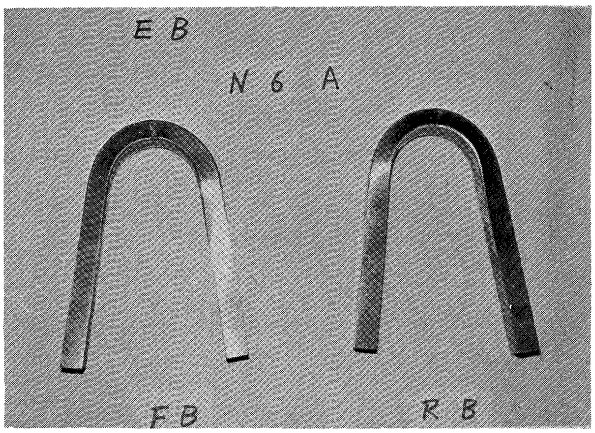

Photo. 3. An example of bend tested specimens.

3.6 Impact test results

1) Testing method

Impact test was performed with standard Charpy 2 mm V notch specimens as shown in Fig. 9 (d). Test specimens were machined from the center of the plate thickness for one pass-welding, and from the first bead for two passes-welding. The center of weld metal, the fusion boundary (we call here "bond") and middle of heat-affected zone ("HAZ") were selected as the notch location of impact test specimens. Six levels of testing temperature, −80, −50, −30, −10, 10 and room temperature (20 to 30°C) were selected in this impact test. Three test specimens were usually tested for each testing temperature.

2) Impact test properties

Transition temperature curves for the absorbed energy for the welds of HT—50, 60 and 80 steels are given in **Figs. 10** through **33.** Furthermore, **Tables 7, 8** and **9** show the transition temperatures of T_{rE} and T_{r15} for HT—50, 60 and 80 steels, respectively.

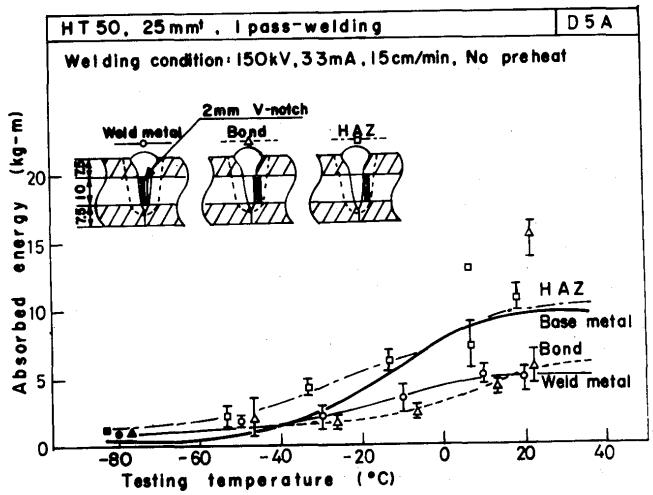

Fig. 10. Transition temperature curve of absorbed energy for welding condition D5A.

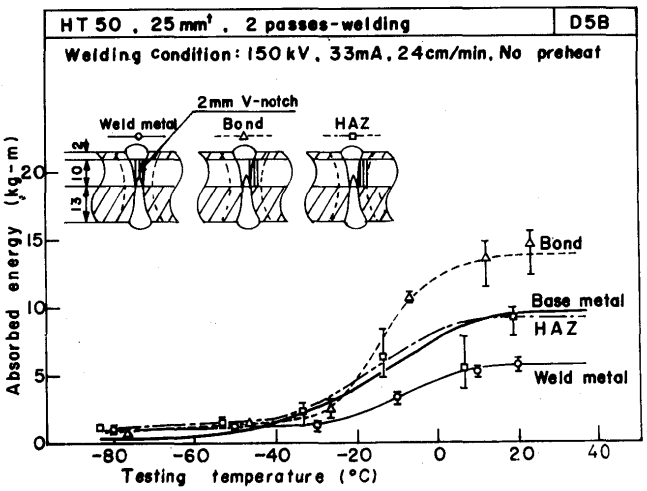

Fig. 11. Transition temperature curve of absorbed energy for welding condition D5B.

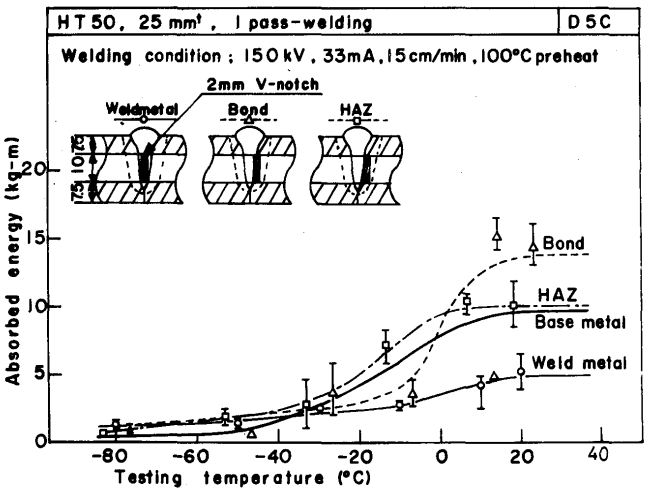

Fig. 12. Transition temperature curve of absorbed energy for welding condition D5C.

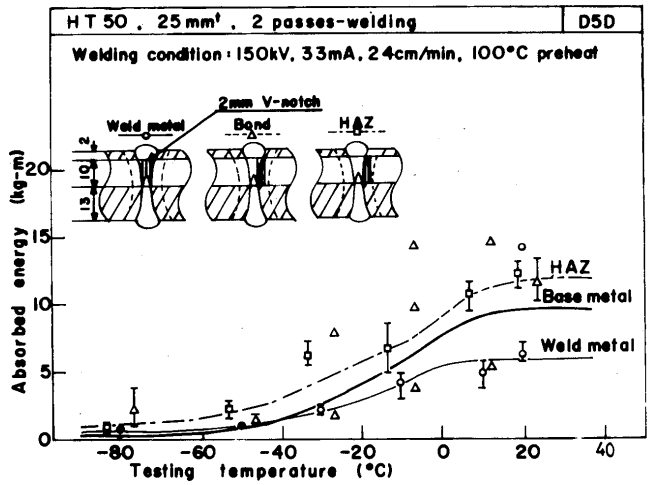

Fig. 13. Transition temperature curve of absorbed energy for welding condition D5D.

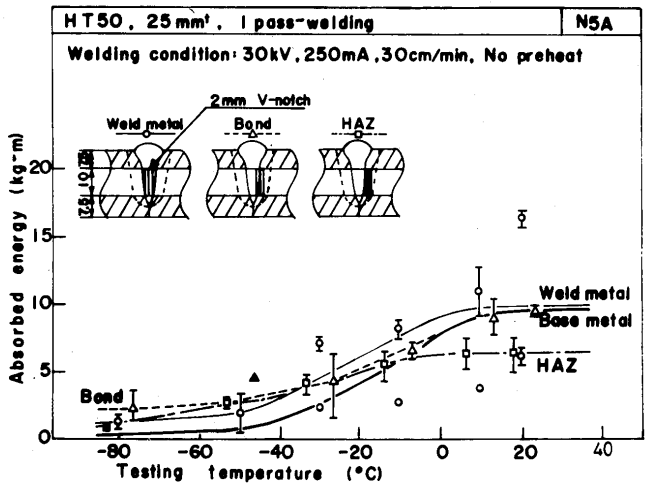

Fig. 14. Transition temperature curve of absorbed energy for welding condition N5A.

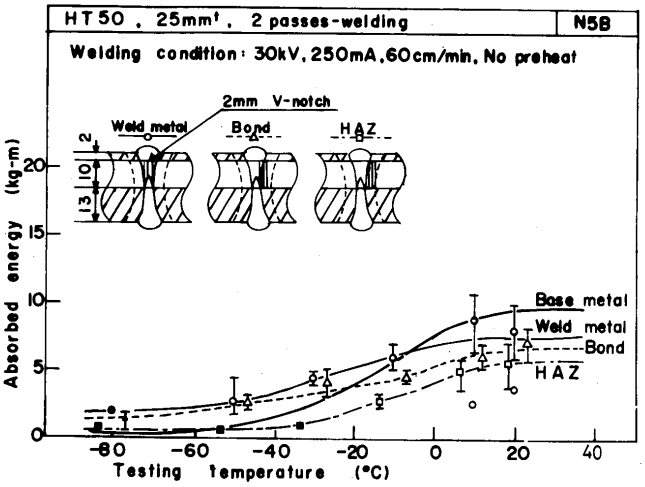

Fig. 15. Transition temperature curve of absorbed energy for welding condition N5B.

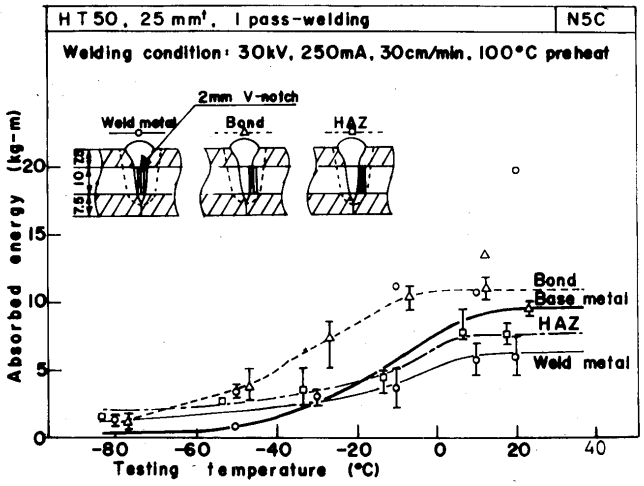

Fig. 16. Transition temperature curve of absorbed energy for welding condition N5C.

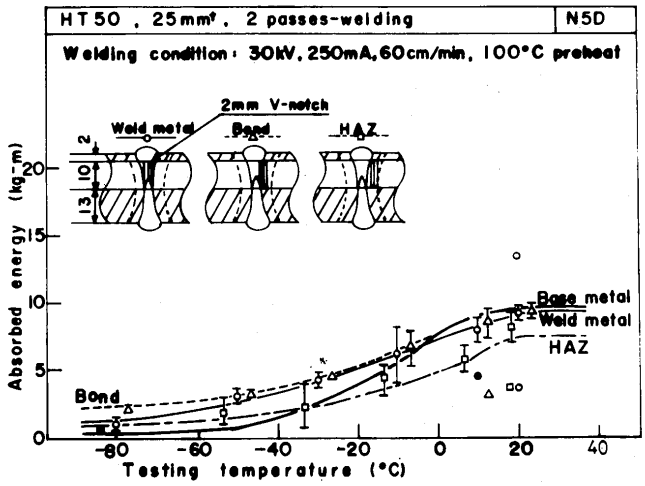

Fig. 17. Transition temperature curve of absorbed energy for welding condition N5D.

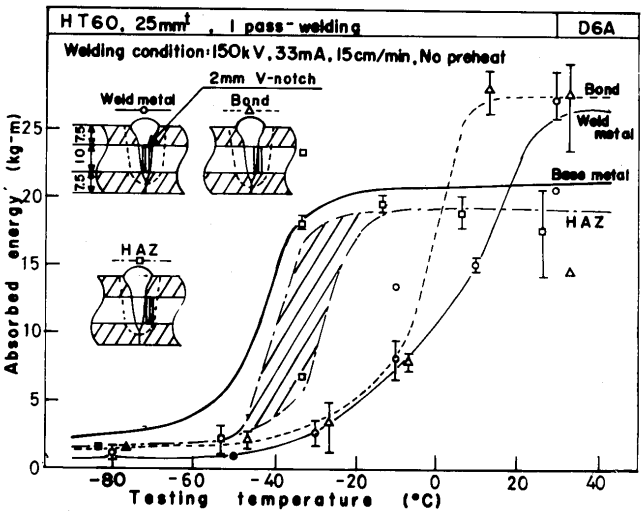

Fig. 18. Transition temperature curve of absorbed energy for welding condition D6A.

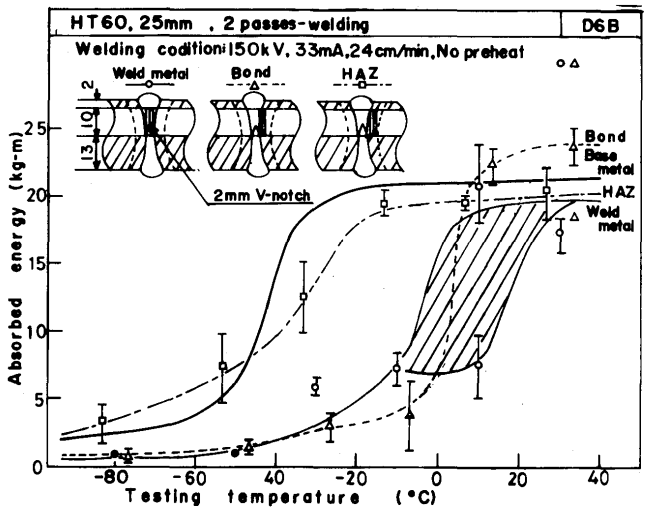

Fig. 19. Transition temperature curve of absorbed energy for welding condition D6B.

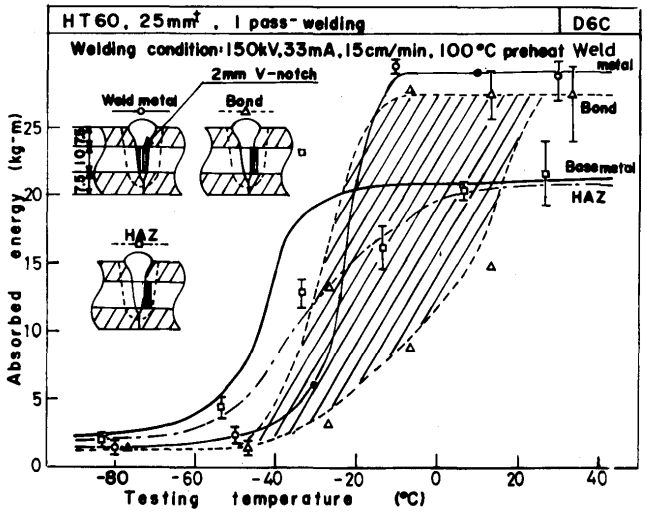

Fig. 20. Transition temperature curve of absorbed energy for welding condition D6C.

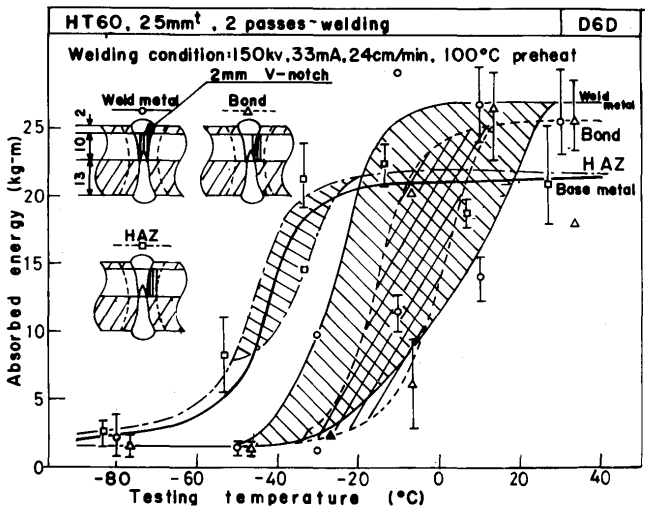

Fig. 21. Transition temperature curve of absorbed energy for welding condition D6D.

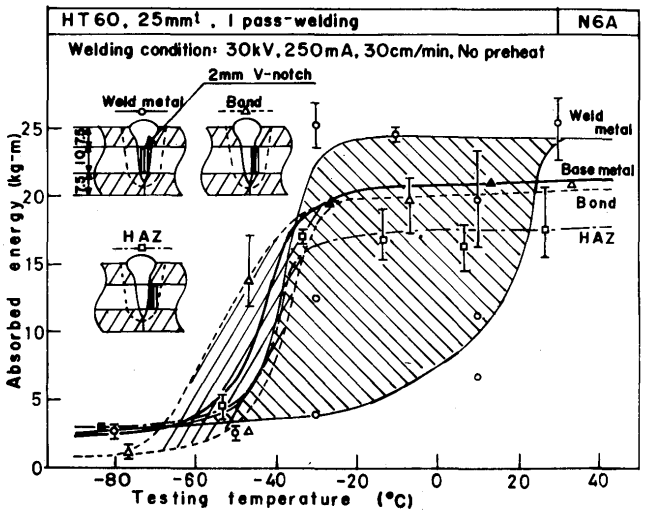

Fig. 22. Transition temperature curve of absorbed energy for welding condition N6A.

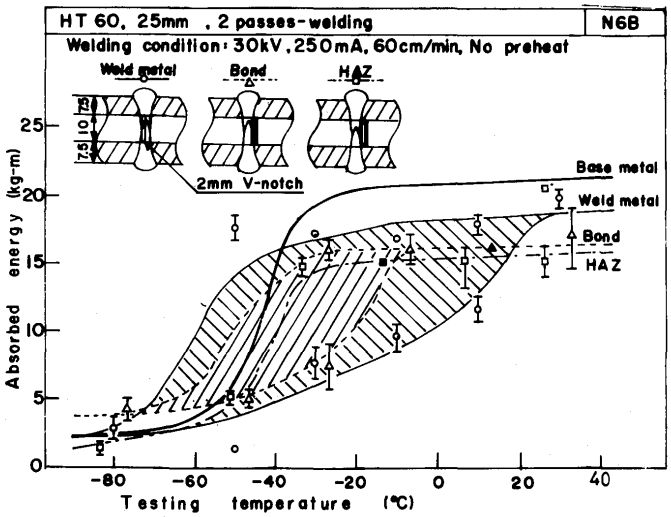

Fig. 23. Transition temperature curve of absorbed energy for welding condition N6B.

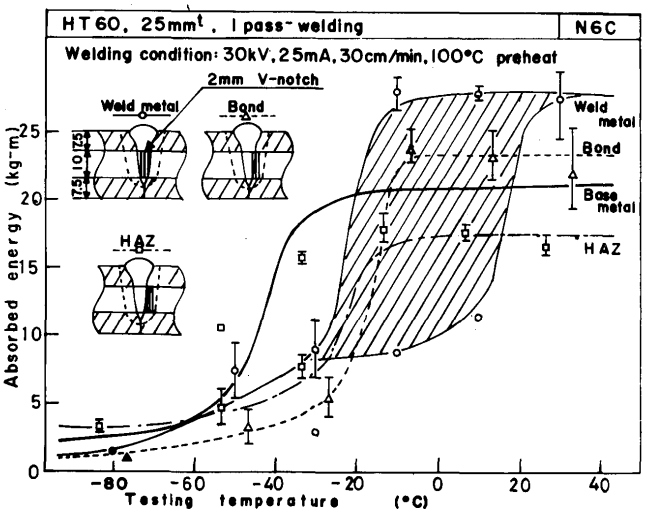

Fig. 24. Transition temperature curve of absorbed energy for welding condition N6C.

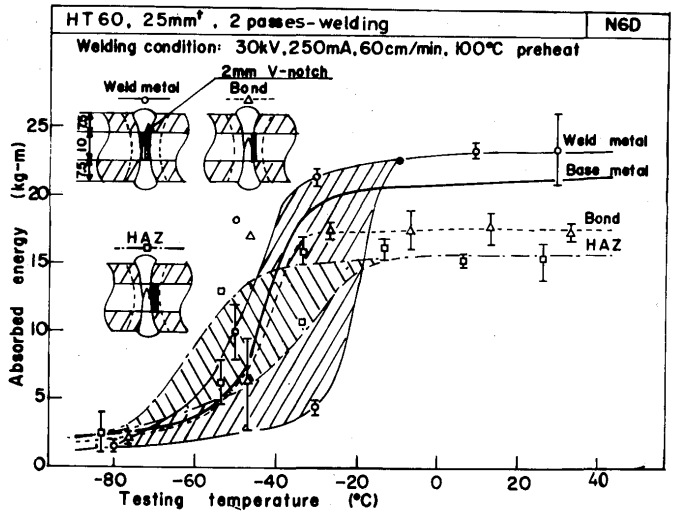

Fig. 25. Transition temperature curve of absorbed energy for welding condition N6D.

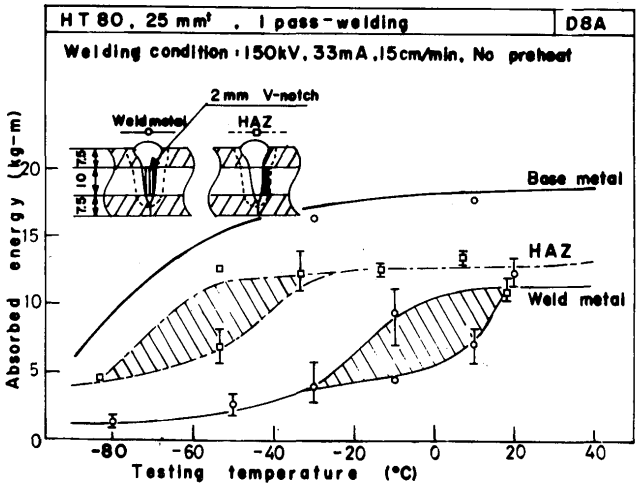

Fig. 26. Transition temperature curve of absorbed energy for welding condition D8A.

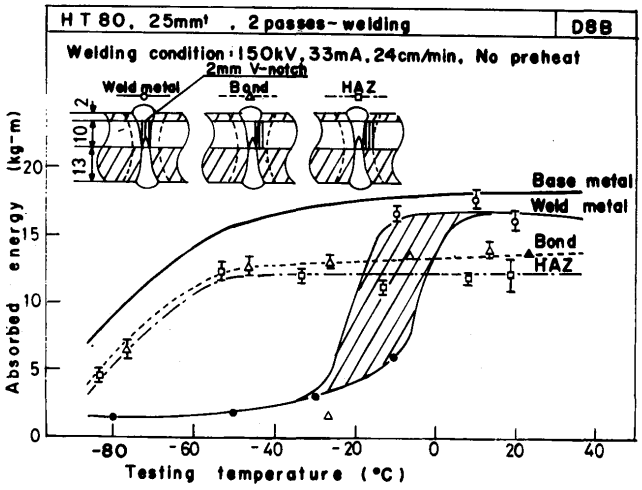

Fig. 27. Transition temperature curve of absorbed energy for welding condition D8B.

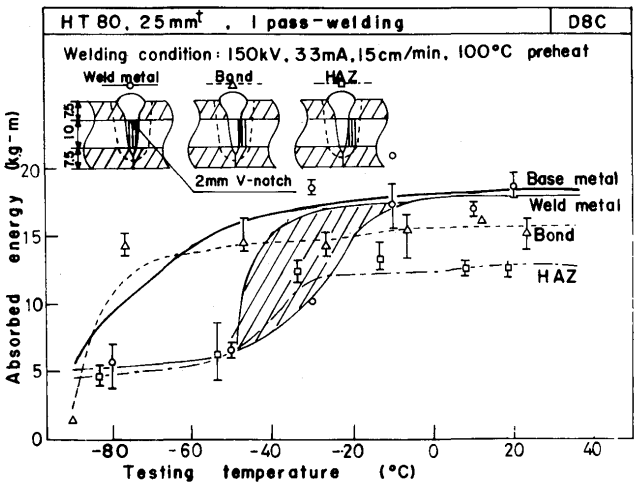

Fig. 28. Transition temperature curve of absorbed energy for welding condition D8C.

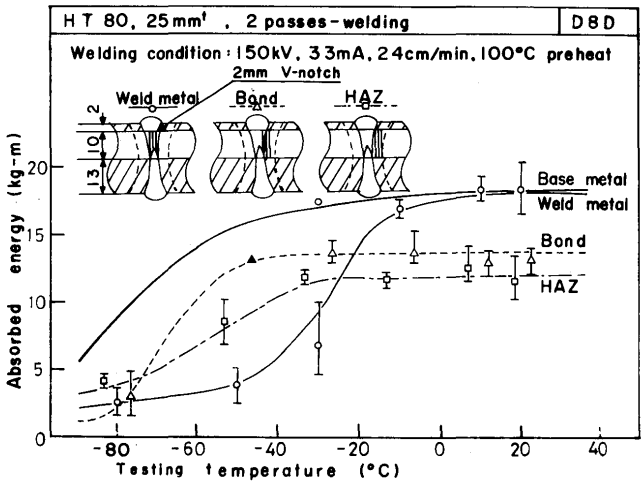

Fig. 29. Transition temperature curve of absorbed energy for welding condition D8D.

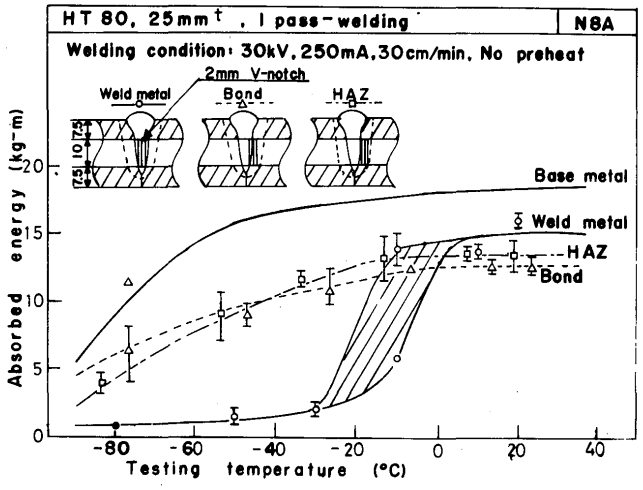

Fig. 30. Transition temperature curve of absorbed energy for welding condition N8A.

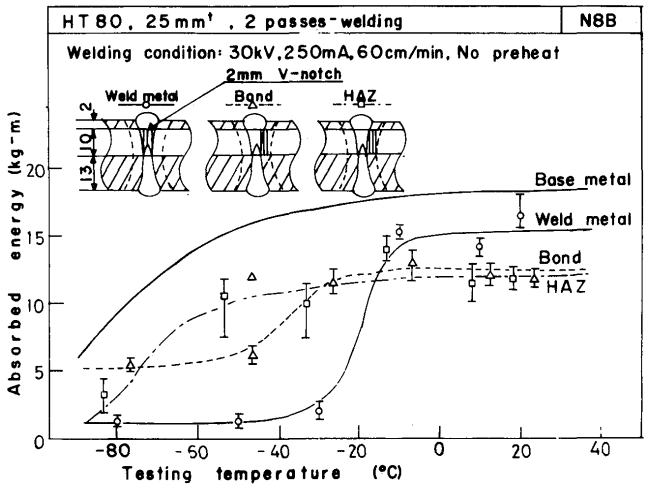

Fig. 31. Transition temperature curve of absorbed energy for welding condition N8B.

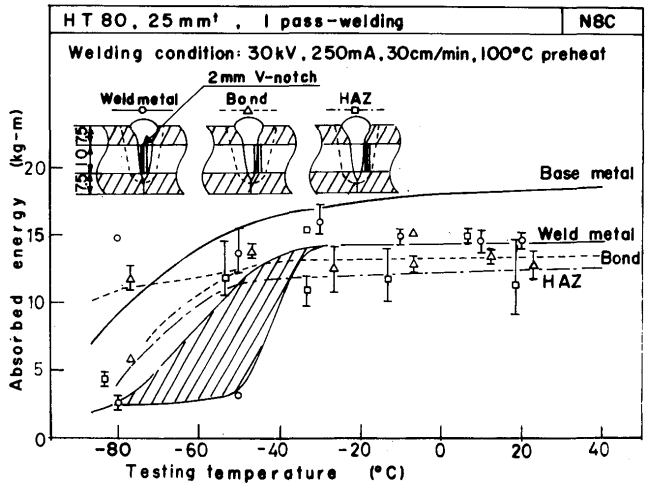

Fig. 32. Transition temperature curve of absorbed energy for welding condition N8C.

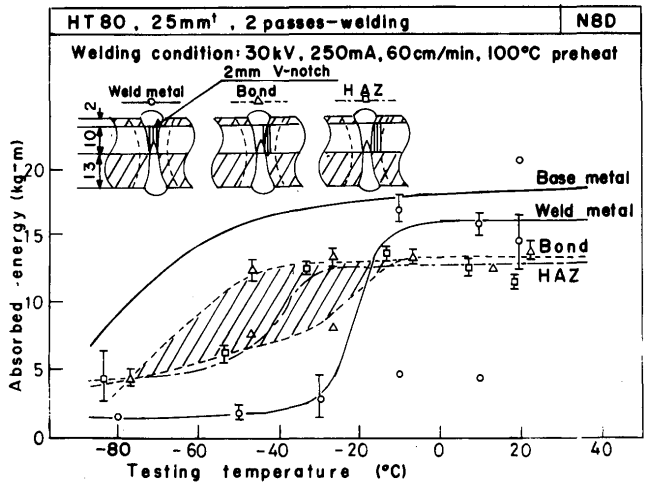

Fig. 33. Transition temperature curve of absorbed energy for welding condition N8D.

3) Study on impact test results

The absorbed energies at R·T for the base metal of HT—50, 60 and 80 steels were about 10, 20 and 18 kg·m, respectively. Impact strength at R·T generally decreased in order of weld metal, bond and HAZ for HT—60 and 80 steels, while it is clearly distinguished in case of HT—50.

In some figures for HT—60 and HT—80, the value of impact strength for weld metal, bond and HAZ at the same temperature frequently showed two levels, the temperature range of which is surrounded by oblique line. It was due to difference in the form of fracture pass in impact specimen as illustrated in **Fig. 34.** When the fracture had propagated straightly along the notched direction as shown in Fig. 34 (a), the absorbed energy showed the low value, however, when the fracture had propagated out the notched direction as shown in Fig. 34 (b), it showed high value.

According to Tables 7, 8 and 9, there are no special relations between weld heat input and T_{rE} and T_{r15}, however it seems that T_{rE} and T_{r15} rise with an increase of weld heat input in case of one pass-welding. Furthermore, T_{rE} and T_{r15} for the weld metal of HT—60 and 80 steels apparently rise in comparison with those of base metal, while in case of HT—50 steels, they have no difference. Nextly it seems that T_{rE} and T_{r15} are not clearly influenced by 100°C preheating, but T_{rE} for the weld metal tends to be improved with 100°C preheating in case of HT—80 steels.

According to JIS and WES Specifications, the minimum absorbed value required in the impact test is prescribed for base metal of HT—50, 60 and 80 steels. The minimum absorbed energies required in these Specifications are tabulated for each steel in **Table 10.** In **Figs. 35** through **37** the relations between the absorbed energy at the specified temperature in JIS and WES and weld heat input are shown. In each figure the minimum absorbed value which prescribed in JIS and WES is shown by the broken line as "Lowest limit". In general it seems that the absorbed energy in the weld metal of HT—50 and 80 steels is gradually decreased with an increase of weld heat input, while

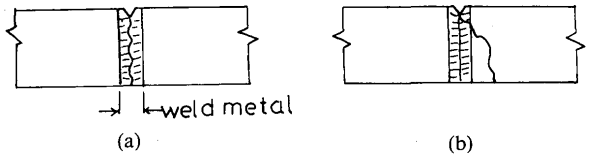

Fig. 34. Difference in form of fracture pass in impact specimen.

Table 7. Summary of transition temperature by V-Charpy impact test of HT—50 welded joint. (Base metal: T_{rE}: −10 (°C), T_{r15}: −35 (°C))

Welding Condition	D5—series												N5—series											
	1 pass-welding (Weld heat input, 20 KJ/cm)						2 passes-welding (12.5 KJ/cm)						1 pass-welding (15 KJ/cm)						2 passes-welding (7.5 KJ/cm)					
Preheating	No			100°C			No			100°C			No			100°C			No			100°C		
Notched Location*	W	B	H	W	B	H	W	B	H	W	B	H	W	B	H	W	B	H	W	B	H	W	B	H
T_{rE}* (°C)	−15	5	−15	−10	0	−20	−10	−15	−20	−15	/	−5	−25	−15	−35	−15	−35	−10	−25	−20	−10	−20	−15	−10
T_{r15}* (°C)	−35	−20	−55	−30	−30	−45	−20	−30	−40	−30	/	−50	−50	−80	−60	−50	−70	−70	−70	−55	−20	−60	−80	−35

* Notched location, W; weld metal B: Bond H; HAZ T_{rE}; Energy transition temp. T_{r15}; 15 f-lb transition temp.

Table 8. Summary of transition temperature by V-Chanpy impact test of HT—60 welded joint. (Base metal: T_{rE}; −45 (°C), T_{r15}; −90 (°C))

Welding Condition	D6-series												N6-series											
	1 pass-welding (Weld heat input, 20 KJ/cm)						2 passes-welding (12.5 KJ/cm)						1 pass-welding (15 KJ/cm)						2 passes-welding (7.5 KJ/cm)					
Preheating	No			100°C			No			100°C			No			100°C			No			100°C		
Notched Location*	W	B	H	W	B	H	W	B	H	W	B	H	W	B	H	W	B	H	W	B	H	W	B	H
T_{rE}* (°C)	−5	5	−40 ~ −30	−25	−30 ~ 5	−30	−5 ~ 15	0	−35	−25 ~ 5	−15 ~ 0	−45 ~ −35	−40 ~ 20	−55 ~ −35	−40	−25 ~ 15	−15	−25	−45 ~ 0	−50 ~ −20	−40	−45 ~ −20	−45	−60 ~ −35
T_{r15}* (°C)	−35	−45	−55	−55	−50 ~ −40	−75	−40 ~ −30	−40	** <−80	−45 ~ −35	−30	<−80	<−80	−75 ~ −55	<−80	−70	−60	<−80	−90	<−80	−70	−75 ~ −60	−80	<−80

*: Notched location, W; Weld metal B; Bond H; HAZ T_{rE}; Energy transition temp. T_{r15}; 15 f-lb transition temp.
**: less than −80 (°C)

Table 9. Summary of transition temperature by V-Charpy impact test of HT—80 welded joint. (Base metal: T_{rE}; −80 (°C), T_{r15}; <−80 (°C))

Welding Condition	D8-series												N8-series											
	1 pass-welding (Weld heat input, 20 KJ/cm)						2 passes-welding (12.5 KJ/cm)						1 pass-welding (15 KJ/cm)						2 passes-welding (7.5 KJ/cm)					
Preheating	No			100°C			No			100°C			No			100°C			No			100°C		
Notched Location*	W	B	H	W	B	H	W	B	H	W	B	H	W	B	H	W	B	H	W	B	H	W	B	H
T_{rE} (°C)	−20 ~ 5	/	−75 ~ −50	−40	−85	−45	−20 ~ −5	−70	−70	−30	−65	−60	−20 ~ −5	−70	−65	−60 ~ −40	−95 ~ −75	−70	−20	−45	−70	−20	−65 ~ −45	−45
T_{r15}* (°C)	−50	/	** <−80	<−80	<−80	<−80	−45	−90	−90	<−80	<−80	<−80	−30	<−80	<−80	−80	<−80	<−80	−35	<−80	<−80	−40	<−80	<−80

*: Notched location, W; Weld metal B; Bond H; HAZ T_{rE}; Energy transition temperature T_{r15}; 15 f-lb transition temperature
**: less than −80 (°C)

in the other parts it has no obvious relation. Furthermore, the impact strength in weld metals of these steels except that of HT—80 with preheating is lower than the others in general. The absorbed energies in HT—60 steel fluctuated widely due to the difference of form of the fracture pass. The value of impact strength for the welds (weld metal, bond and HAZ) of HT—60 and 80 steels is exceeding the lowest limit in JIS and WES Specifications, however in case of HT—50 steel it is not always enough to these Specifications, and some of welds show the value less than WES' limit. The reason is thought that the absorbed energy in the base metal of HT—50 is rather low and is near the lowest limit.

4. Conclusion

(1) Elimination of the scale, cleaning of the contamination for the joints and de-magnetization must be completely performed before electron-beam welding in order to make the defect-free weld metals of HT—50, 60 and 80 steels. The defect-free weld metals

Table 10. The minimum absorbed energy required in V-notched impact test specimen in JIS and WES Specifications.

Specification \ Materials	Materials	HT—50	HT—60	HT—80
JIS* G3106—1973	Corresponding	SM50B	SM58	HW70
	T· S (kg/mm²)	50~62	58~73	80~95
	Temp. (°C)	0	−5	−15
	Absorbed energy (kg·m)	>2.8	>4.8	>3.6
WES* 135—1961	Corresponding material	HW36	HW45	HW80
	T· S (kg/mm²)	53~65	60~72	80~95
	Temp. (°C)	0	−5	−15
	Absorbed energy (kg·m)	>4.8	>4.8	>3.6

* JIS; Japan Industrial Standard
WES; Welding Engineering Standard

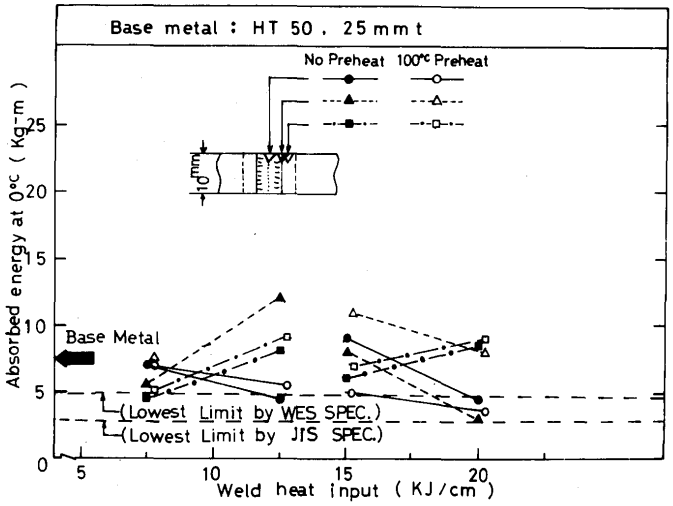

Fig. 35. Relation between absorbed energy of HT—50 at specified temperature in JIS and WES and weld heat input.

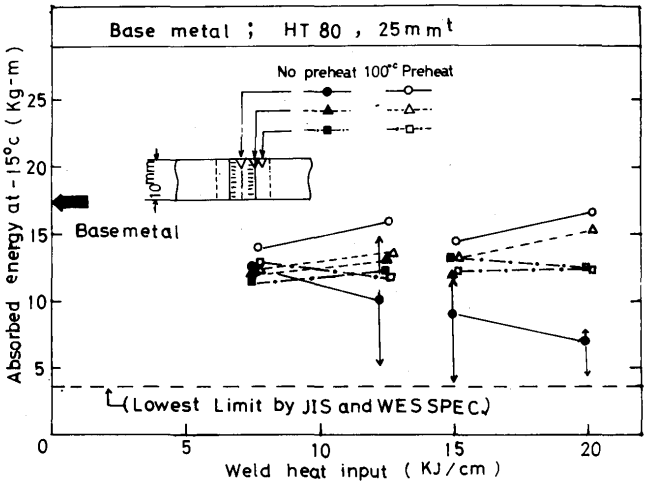

Fig. 37. Relation between absorbed energy of HT—80 at specified temperature in JIS and WES and weld heat input.

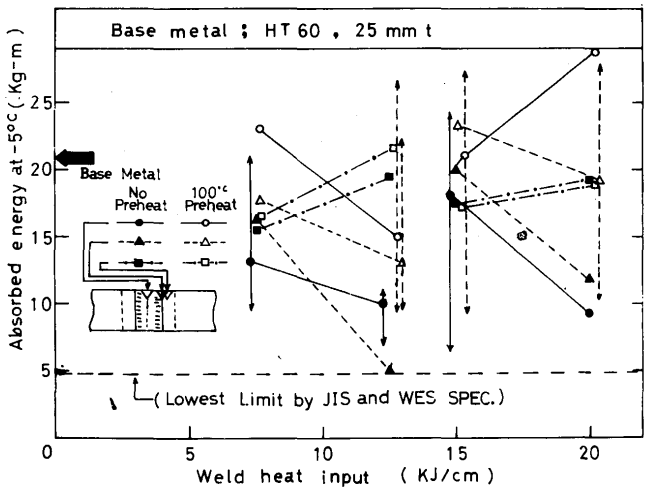

Fig. 36. Relation between absorbed energy of HT—60 at specified temperature in JIS and WES and weld heat input.

which were inspected by X-ray and dye penetrant inspections were obtained for these steels in this experiment.

(2) According to quantitative analysis for weld metal, it seems that there is a little vaporization of Mn element in weld metal.

(3) Judging from the microphotographs of the welds, 100°C preheating has no notable effect upon the variation of microstructures in the weld metal of HT—50, 60 and 80 steels. However, as the welding speed decreases, the cells which grow parallel to the welding direction are obviously observed.

(4) Microhardness of welds

(a) The hardness in weld metal is usually softer than that in the HAZ. This reason is considered due to reduction of Mn element in weld metal.

(b) The hardness of welds for both one pass and two passes-welding are reduced with 100°C preheating.

(c) The hardnesses of welds are reduced with an increase of weld heat input regardless of high and low voltage type electron-beam welders.

(d) The bottom part of a weld penetration for one pass-welding shows harder in hardness than the surface part.

(5) The tensile tested specimens of electron-beam welded joints of HT—50, 60 and 80 steels showed sound properties and were mostly fractured in base metal.

(6) All of the face and the root bend tested specimens of electron-beam welded joints of HT—50, 60 and 80 steels showed a complate bend angle of 180 degrees without serious defects.

(7) Impact tests by standard V-Charpy test specimen

(a) Absorbed energies for the base metal of HT—50, 60 and 80 steels are about 10, 20 and 18 kg·m at room temperature, respectively. T_{rE} and T_{r15} for the weld metal of HT—60 and 80 steels apparently rise in comparison with those of respective base metal, while in case of HT—50 steels, no obvious difference is observed between them.

(b) T_{rE} and T_{r15} for the welds of these steels had no obvious relations with weld heat input, however they tended to rise with an increase of weld heat input for one pass-welding, and then they were not clearly influenced with 100°C preheating.

(c) In case of the electron-beam welds of HT—60 and 80 steels, the absorbed energies of weld metal, bond and HAZ are usually exceeding the minimum absorbed energy required in JIS and WES Specifications, even though they showed lower value than that of base metal. In case of HT—50, however, the absorbed energies in weld metal, bond and HAZ are not always satisfied with criteria of WES.

Acknowledgement

The authors wish to acknowledge the co-operative support of Japan Electron Optics Industries and Osaka Transformer Co. Ltd.

References

1) H. I. Mchenry et al: "Electron Beam Welding of D6AC Steels", Welding Journal, Vol. 45, No. 9, Sep., 419S–425S, 1966.

2) A. J. Williams et al: "Properties of Electron-Beam Welds in Ultra-High-Strength Steels", 1st International Conference of Electron and Ion Beam Science and Technology, 1965, 674~712.

3) Y. Arata et al: "Study on Characteristics of Weld Defect and Its Prevention in Electron Beam Welding (Report I)", Trans. of JWRI, Vol. 2, No. 1, p. 103~112, 1973.

4) F. Matsuda et al: "Some Metallurgical Investigations on Electron-Beam Welds", Trans. of JWS, Vol. 1, No. 1, p. 72~85, 1970.